



# Geometrical Influence on Stability of FGM Beams under Vibration

S. N. Padhi, K. S. Raghu Ram, G. Bhavani, K. Suresh, V. V. K. Lakshmi, T. Rout

**Abstract:** In this paper the influence of geometry on the stability of a functionally graded material rotating beam is reported. The equation of motion is formulated using Hamilton's principle in association with finite element analyses. Floquet's theory was used for establishing the stability boundaries. The properties of functionally graded ordinary (FGO) and functionally graded sandwich (FGSW) beams under consideration are assumed to be graded following either power law or exponential law across the thickness of the beam. The effect of geometry in terms of slenderness parameter on the dynamic stability of both FGO & FGSW beams have been investigated. The increase in slenderness parameter enhances the stability of both the FGO and FGSW beams. Further it has been observed that exponential distribution of properties ensures better stability compared to power law distribution of properties.

**Index Terms:** Power law, Exponential distribution, FGO beam, FGSW beam, Slenderness parameter, Stability.

## I. INTRODUCTION

The engineering materials can be classified into three primary classes: metals and alloys; ceramics and glasses; and polymers. Among these three primary classes, metals, metallic alloys, and polymers are more widely implemented in various structural and engineering applications than ceramics and glasses. Somehow, ceramics have also drawn considerable attention from the scientific community in last three decades. Depending on whether metals, ceramics, or polymers comprise more than 50% by volume of a composite, it can further be classified as a Metal Matrix Composite (MMC), a Ceramic Matrix Composite (CMC), or a Polymer Matrix Composite (PMC), respectively [1].

The composites have a typical nature that is they neither dissolve nor blend into each other. By this way we can easily identify the constituents of the composite. Their strength and stiffness is an added benefit along with the light weight. Here Matrix is the material which protects as the reinforcements and also serves to bind [2]. Production of hybrid aluminium materials is presented in this paper.

Aluminium metal matrix composites and methods of fabrication of hybrid composites in the recent years is increasing in usage for commercial and industrial applications both under static and dynamic conditions. Conventional materials are easy to manufacture and machine, where as hybrid materials require unconventional machining processes which are hard to machine by traditional methods or almost results in unproductive machining. Aeronautical, military, medical, opto electronics and many other industries are replacing conventional aluminium material and employing hybrid aluminium [3,6]. Glass fiber reinforced composites are widely used in industries for the development of high-end applications such as automotive spare parts, aerospace because of their ability to withstand high tensile, flexural and impact loads. uralumin has excellent strength to weight ratio, having a good strength while being lightweight. Duralumin was casted by taking its standard composition of aluminium, copper, magnesium, manganese and silicon [4,9]. The aluminum fly ash metal matrix composites (MMCs) find wide applications in automobile and aerospace which require high strength and modulus. This present article attempts to highlight the fly ash management to make use of this solid waste, the fly ash, in order to save our environment and produce goods at economic cost. The present report is to carry out a detailed techno market evaluation regarding various high value added products and applications of fly ash with a view to identify the viable technologies those are available to India and determine the market potential of these technologies within existing constraints. The fly ash which is a byproduct of coal burning especially from thermal power plants is being used as reinforcement for MMCs due to its low cost and reduction in environmental pollution [5,10]. Aluminium matrix composites (AMCs) are the competent material in the industrial world. Due to the excellent mechanical properties, these AMCs are widely used in fgetting strengthened when it is reinforced with the hard ceramic particles like  $Al_2O_3$  and  $B_4C$  etc. Aluminium alloys are still the subjects of intense studies, as their low density gives additional advantages in several applications [7]. The primary advantage of modern composite materials is that they are both strong and light. By choosing a correct matrix mix and reinforcement material, a new material can be generated that meets the precise requirements of a particular implementation. As many can be molded into complex forms, a composite also offers flexibility in design [8].

The major issues in conventional laminated composite materials, such as debonding, huge residual stress, locally large plastic deformations can be eliminated by using FGM. An FGM can be made as a good substitute for the rotating beam material.

**Revised Manuscript Received on February 28, 2020.**

\* Correspondence Author

**Surya Narayan Padhi\***, Department of Mechanical Engg., Koneru Lakshmaiah Education Foundation, Guntur, India.

**K. S. Raghu Ram**, Department of Mechanical Engg., Vignan's Institute of Information Technology, Visakhapatnam, India.

**G. Bhavani**, Department of Mechanical Engg., Vignan's Institute of Information Technology, Visakhapatnam, India.

**K. Suresh**, Department of Mechanical Engg., GIT, GITAM.

**V. V. K. Lakshmi**, Department of Mechanical Engg., GIT, GITAM.

**Trilochan Rout**, Department of Mechanical Engg., Parala Maharaja Engineering College, Berhampur, India.

© The Authors. Published by Blue Eyes Intelligence Engineering and Sciences Publication (BEIESP). This is an [open access](http://creativecommons.org/licenses/by-nc-nd/4.0/) article under the CC-BY-NC-ND license <http://creativecommons.org/licenses/by-nc-nd/4.0/>

Functionally Graded Sandwiched structures find their use in spacecrafts, machinery and automobile industries because they have their high strength and stiffness compared to their low weight. In modern engineering, the FGSW beams have gradually substituted the large weighed metallic beams.

Rotating FGSW beam structures are commonly found in engineering applications, including robotics, turbine blades, and helicopter rotors. Vibration of rotating structures has become a commonly occurring phenomenon [11]. The buckling behavior of size-dependent microbeams made of functionally graded materials (FGMs) for different boundary conditions is investigated on the basis of Bernoulli–Euler beam and modified strain gradient theory. The effects of the power of the material property variation function, boundary conditions, slenderness ratio, ratio of additional material length scale parameters for two constituents, beam thickness-to-additional material length scale parameter ratio on the buckling response of FGM microbeams are investigated [12]. Thermal stability analysis of circular functionally graded sandwich plates of variable thickness using pseudo-spectral method researches have done on the subject of buckling and post-buckling of FGM plates of constant thickness. However, the subject of FGM plates with variable thickness has been taken under advisement by researchers [13]. An FGM can be a good replacement for the material of rotating beams. The research on functionally graded materials (FGMs) is rapidly growing because of its ability to meet desired material properties in contrast to the conventional homogeneous and layered composite materials which suffer from debonding, huge residual stress, locally large plastic deformations etc. [14,16]. Analytical solutions of natural frequencies and critical buckling load are obtained for cracked FGM beams with clamped-free, hinged-hinged, and clamped-clamped end supports. A detailed parametric study is conducted to study the influences of crack depth, crack location, total number of cracks, material properties, beam slenderness ratio, and end supports on the free vibration and buckling characteristics of cracked FGM beams [15]. The equations, including a material length scale parameter as well as a nonlocal parameter, can describe the size-dependent in linear and nonlinear vibration of FGM nanotubes. Analytical solution is obtained by using a two-steps perturbation method. Eventually, the effects of various physical parameters on nonlinear and linear natural frequencies of FGM nanotubes are analyzed, such as inner radius, temperature, nonlocal parameter, strain gradient parameter, scale parameter ratio, slenderness ratio, volume indexes, different beam models [17,19]. Many machine and structural components in aforesaid sections can be modeled as rotating beams. These rotating beam structural members may undergo forced vibration and dynamic instability during their service period, which may even lead to their failure. So the study of effect of the system parameters on free vibration behavior of FGO and FGSW beams forms an important aspect of investigation [18].

Although many papers have been published on different parameters effecting the static and dynamic stability of ordinary beams, the literature on effect of geometry on dynamic stability of functionally graded rotating beams have hardly been found. Hence an attempt has been made to

findout the influence of slenderness parameter on the stability of FGO & FGSW rotating cantilever beams.

## II. FORMULATION

A beam of functionally graded material sandwiched between top skin and bottom skin respectively as alumina and steel is shown in Fig. 1(a). The beam is made free at one end and fixed at the other end. The sandwiched beam is subjected to a time varying axial force  $P(t) = P_s + P_t \cos \Omega t$ , and acting along its undeformed axis having  $P_s$  and  $P_t$  respectively the static component of the axial force, and amplitude.  $\Omega$  is the frequency of load and  $t$  is the time. Fig. 1(b) shows a two noded finite element coordinate system used to derive the governing equations of motion. The thickness coordinate is measured as 'z' from the reference plane. The axial displacement and the transverse displacement of a point on the reference plane are  $u$  and  $w$  respectively and  $\phi$  is rotation of cross-sectional plane with respect to the un-deformed configuration. Figure 1(c) shows a two-nodded beam finite element having three degrees of freedom per node.

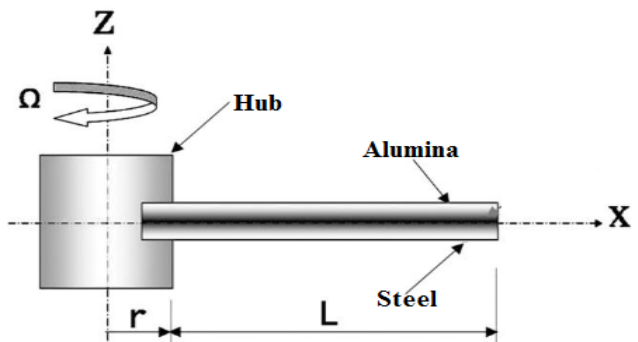


Figure 1(a) FGSW beam subjected to dynamic axial load.  $Z, w, V_z$

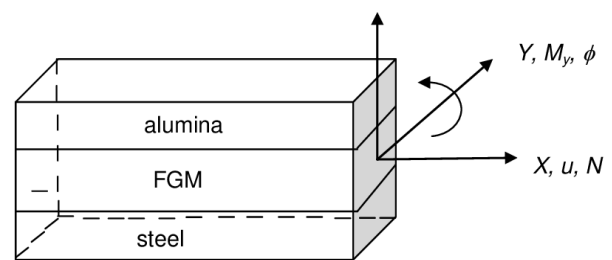


Figure 1(b) The coordinate system with generalized forces and displacements for the FGSW beam element.

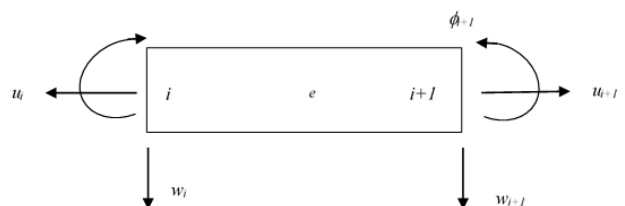


Figure 1(c) Beam element showing generalized degrees of freedom for ith element.

### A. Shape Functions

According to the first order Timoshenko beam theory the displacement fields are expressed as

$$U(x, y, z, t) = u(x, t) - z\phi(x, t),$$

$$W(x, y, z, t) = w(x, t), \quad (1)$$

Where  $U$  = axial displacement and  $W$  = transverse displacement of a material point. The respective linear strains are

$$\epsilon_{xx} = \frac{\partial u}{\partial x} - z \frac{\partial \phi}{\partial x}, \quad \gamma_{xz} = -\phi + \frac{\partial w}{\partial x} \quad (2)$$

The matrix form of stress-strain relation is

$$\{\sigma\} = \begin{Bmatrix} \sigma_{xx} \\ \tau_{xz} \end{Bmatrix} = \begin{bmatrix} E(z) & 0 \\ 0 & kG(z) \end{bmatrix} \begin{Bmatrix} \epsilon_{xx} \\ \gamma_{xz} \end{Bmatrix} \quad (3)$$

Where  $\sigma_{xx}, \tau_{xz}, E(z), G(z)$  and  $k$  are the normal stress on x-x plane, shear stress in x-z plane, Young's modulus, shear modulus and shear correction factor respectively. The variation of material properties along the thickness of the FGM beam governed by

(i) Exponential law is given by

$$M(z) = M_t \exp(-e(1 - 2z/h)) \quad (4)$$

$$e = \frac{1}{2} \log \left( \frac{M_t}{M_b} \right), \text{ and}$$

(ii) Power law is given by

$$M(z) = (M_t - M_b) \left( \frac{z}{h} + \frac{1}{2} \right)^n + M_b \quad (5)$$

Where,  $M(z)$  can be any one of the material properties such as,  $E, G$  and  $\rho$  etc., denote the values of The corresponding properties at top and bottommost layer of the beam are represented by  $M_t$  and  $M_b$  respectively, and the power index is  $n$ .

Now the shape function can be expressed as

$$\mathfrak{N}(x) = [\mathfrak{N}_u(x) \quad \mathfrak{N}_w(x) \quad \mathfrak{N}_\phi(x)]^T \quad (6)$$

where,  $\mathfrak{N}_u(x), \mathfrak{N}_w(x), \mathfrak{N}_\phi(x)$  are the shape functions for the axial, transverse and rotational degree of freedom respectively.

### B. Element Elastic Stiffness Matrix

The element elastic stiffness matrix is given by the relation

$$[k_e] \{\hat{u}\} = \{F\} \quad (7)$$

where,  $\{F\}$  = nodal load vector and  $[k_e]$  = element elastic stiffness matrix.

### C. Element Mass Matrix

The element mass matrix is given by

$$T = \frac{1}{2} \{\hat{u}\}^T [m] \{\hat{u}\} \quad (8)$$

### D. Element Centrifugal Stiffness Matrix

The  $i$ th element of the beam is subjected to centrifugal force which can be expressed as

$$F_c = \int_{x_i}^{x_i+l} \int_{-h/2}^{h/2} b\rho(z) \tilde{N}^2 (R+x) dz dx \quad (9)$$

Where  $x_i$  = the distance between  $i^{\text{th}}$  node and axis of rotation,  $\tilde{N}$  and  $R$  are the angular velocity and radius of hub. Work due to centrifugal force is

$$W_c = \frac{1}{2} \int_0^l F_c \left( \frac{dw}{dx} \right)^2 dx = \frac{1}{2} \{\hat{u}\} [k_c] \{\hat{u}\} \quad (10)$$

Where,

$$[k_c] = \int_0^l F_c [\mathfrak{N}'_w]^T [\mathfrak{N}'_w] dx \quad (11)$$

### E. Element Geometric Stiffness Matrix

The work done due to axial load  $P$  may be written as

$$W_p = \frac{1}{2} \int_0^l P \left( \frac{\partial w}{\partial x} \right)^2 dx \quad (12)$$

Substituting the value of  $w$  from eq. (6) into eq. (12) the work done can be expressed as

$$W_p = \frac{P}{2} \int_0^l \{\hat{u}\}^T [\mathfrak{N}'_w]^T [\mathfrak{N}'_w] \{\hat{u}\} dx = \frac{P}{2} \{\hat{u}\} [k_g] \{\hat{u}\} \quad (13)$$

here,

$$[k_g] = \int_0^l [\mathfrak{N}'_w]^T [\mathfrak{N}'_w] dx \quad (14)$$

Where,  $[k_g]$  = geometric stiffness matrix of the element.

## III. EQUATION OF MOTION

Using Hamilton's principle.

$$\delta \int_{t_1}^{t_2} (T - S + W_p - W_c) dt = 0 \quad (15)$$

Substituting Eqns (7, 8, 10 and 13) into Eqn (15) and rewritten in Eqn (16)

$$[m] \{\hat{u}\} + [[k_t] - P(t)[k_g]] \{\hat{u}\} = 0 \quad (16)$$

$$[M]\{\ddot{U}\} + \left[ [K_t] - P^\oplus (\alpha + \beta_d \cos \Omega t) [K_g] \right] \{U\} = 0 \quad (17)$$

$$[K_t] = [k_e] + [k_c] \quad (18)$$

where,  $[k_e]$ ,  $[k_c]$ ,  $[m]$  and  $[k_g]$  are elastic stiffness matrix, centrifugal stiffness matrix, mass matrix and geometric stiffness matrix respectively.  $[K_t]$  is the total stiffness matrix. Assembling the element matrices as used in eq. (17), the equation of motion in global matrix form for the beam, can be expressed as

$$[M]\{\ddot{U}\} + \left[ [K_t] - P^\oplus (\alpha + \beta_d \cos \Omega t) [K_g] \right] \{U\} = 0 \quad (19)$$

Where  $[M]$ ,  $[K_t]$ ,  $[K_g]$  are global mass, total stiffness and geometric stiffness matrices respectively and  $\{U\}$  is global displacement vector. Equation (19) represents a system of second order differential equations with periodic coefficients of the MathieuHill type. Floquet Theory has been used to distinguish between the dynamic stability and instability zones as follows. A solution with period  $2T$  which is of practical importance is represented by

$$\hat{U}(t) = c_1 \sin \frac{\Omega t}{2} + d_1 \cos \frac{\Omega t}{2} \quad (20)$$

Substituting eq. (20) into eq. (19) and solving the boundary solutions with period  $2T$ . The resulting equation is given by

$$\left( [K_t] - (\alpha \pm \beta_d / 2) P^\oplus [K_g] - \frac{\Omega^2}{4} [M] \right) \{U\} = 0 \quad (21)$$

Equation (21) ends up with an eigenvalue problem with known quantities  $P^\oplus$ ,  $\alpha$ ,  $\beta_d$ . Where  $P^\oplus$  is the critical buckling load.

The plus and minus sign in the eq. (21) results with two sets of eigenvalues ( $\Omega$ ) binding the regions of instability and can be determined from the solution of the above equation

$$\left| [K_t] - (\alpha \pm \beta_d / 2) P^\oplus [K_g] - \frac{\Omega^2}{4} [M] \right| = 0 \quad (22)$$

#### A. Free Vibration

The eq. (22) can be written for a problem of free vibration by substituting  $\alpha = 0$ ,  $\beta_d = 0$ , and  $\omega = \frac{\Omega}{2}$

$$\left| [K_t] - \omega^2 [M] \right| = 0 \quad (23)$$

The values of the natural frequencies  $\{\omega\}$  can be obtained by solving eq. (23).

#### B. Static Stability

The eq. (22) can be written for a problem of static stability by substituting  $\alpha = 1$ ,  $\beta_d = 0$ , and  $\omega = 0$

$$\left| [K_t] - P^\oplus [K_g] \right| = 0 \quad (24)$$

The values of buckling loads can be obtained by solving eq. (24).

#### C. Regions of Instability

$\omega_1$  and  $P^\oplus$  are calculated from eq. (23) and eq. (24) for an isotropic steel beam with identical geometry and end conditions ignoring the centrifugal force.

Choosing  $\Omega = \left( \frac{\Omega}{\omega_1} \right) \omega_1$ , eq. (22) can be rewritten as

$$\left| [K_t] - (\alpha \pm \beta_d / 2) P^\oplus [K_g] - \left( \frac{\Omega}{\omega_1} \right)^2 \frac{\omega_1^2}{4} [M] \right| = 0 \quad (25)$$

For fixed values of  $\alpha$ ,  $\beta_d$ ,  $P^\oplus$ , and  $\omega_1$ , the eq. (25) can

be solved for two sets of values of  $\left( \frac{\Omega}{\omega_1} \right)$  and a plot between

$\beta_d$  and  $\left( \frac{\Omega}{\omega_1} \right)$  can be drawn which will give the zone of dynamic instability.

### IV. RESULTS AND DISCUSSION

In the present analyses a steel-alumina functionally graded ordinary (FGO) and functionally graded sandwich (FGSW) rotating cantilever beams are taken for the parametric instability. The beams are steel-rich bottom and alumina-rich top. The mechanical properties of the two phases of the beam are considered as given in the following table [11].

**Table 1. Material properties of Steel-Alumina FGO beam.**

Material	Properties		
	Young's modulus E	Shear modulus G	Mass density $\rho$
Steel	$2.1 \times 10^{11}$ Pa	$0.8 \times 10^{11}$ Pa	$7.85 \times 10^3$ kg/m <sup>3</sup>
Alumina	$3.9 \times 10^{11}$ Pa	$1.37 \times 10^{11}$ Pa	$3.9 \times 10^3$ kg/m <sup>3</sup>
Poisson's ratio $\nu$ is assumed as 0.3, shear correction factor $k = (5 + \nu) / (6 + \nu) = 0.8667$			
Static load factor $\alpha = 0.1$			
Critical buckling load, $P^\oplus = 6.49 \times 10^7$ N			
Fundamental natural frequency $\omega_1 = 1253.1$ rad/s			

The value of slenderness parameter, hub radius parameter, angular speed parameter are used as 0.2, 0.1 and 1.15 respectively unless they are specified.

The length of the beam is denoted by  $L$ .

Hub radius parameter  $\delta = \frac{R}{L}$ , Rotary inertia parameter

$$r = \frac{1}{L} \sqrt{\frac{I}{A}},$$



$$\text{Frequency parameter } \eta_n = \sqrt{\frac{\rho A L^4 \omega_n^2}{EI}}$$

The area moment of inertia of the cross section about the centroidal axis is  $I$ , the  $n^{\text{th}}$  mode frequency of the beam is  $\omega_n$  and  $\eta_n$  is the  $n^{\text{th}}$  mode frequency parameter.

The following additional non-dimensional parameters are chosen for the analysis of the beam.

Slenderness parameter  $s = h/L$

$$\text{Rotational speed parameter } \nu = \sqrt{\frac{\rho A L^4 \tilde{N}^2}{EI}}$$

$\tilde{N}$  is the rotational speed in rad/s

$E$ ,  $G$  and  $\rho$  are the Young's modulus, shear modulus and mass density of steel respectively and their values are given in the following section.

### A. Functionally graded ordinary beam

A steel-alumina functionally graded ordinary (FGO) rotating cantilever beam of length 1m and width 0.1m is considered for the analysis of parametric instability. The influence of geometry measured by the slenderness parameter ( $s$ ) according to power law with index  $n=2.5$  (FGO-2.5) and according to exponential law (e-FGO) are considered for dynamic stability analysis.

The role of geometry of the beam on the first and second mode instability zones of FGO-2.5 beam is presented in Fig. 2(a) and 2(b) respectively. The area of instability zone becomes narrower and shifts away from the dynamic load factor axis as the slenderness parameter ( $s$ ) increases thereby enhancing the stability of the beam. The effect of slenderness parameter on stability of e-FGO beam is similar as on FGO-2.5 beam which can be noticed from Fig. 2(c) and 2(d) respectively for first and second modes.

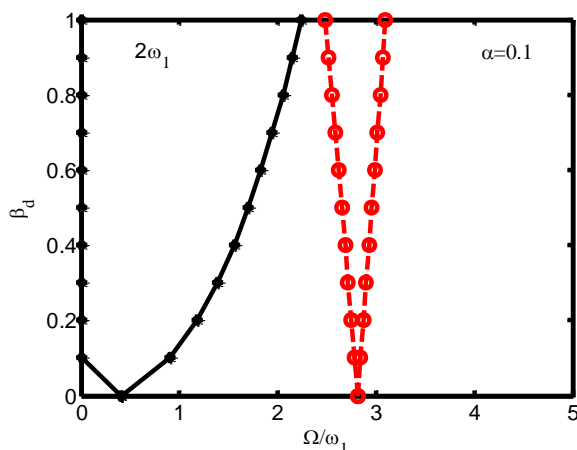


Figure 2(a). Effect of slenderness parameter on first mode instability region of steel-alumina FGO beam for  $n=2.5$ ,  $\delta=0.1$ ,  $\tilde{N}=344$  rad/s (\*  $s=0.1$ ,  $o^s=0.3$ )

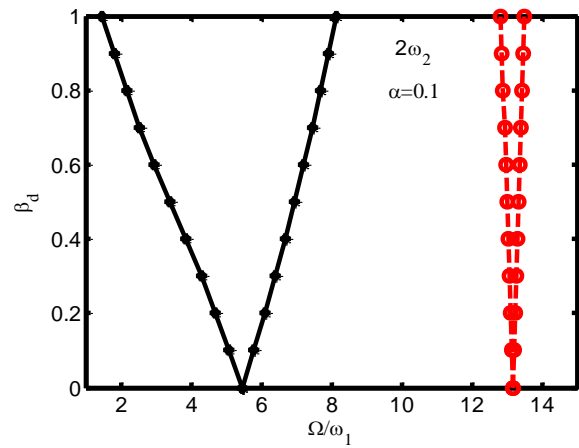


Figure 2(b). Effect of slenderness parameter on second mode instability region of steel-alumina FGO beam for  $n=2.5$ ,  $\delta=0.1$ ,  $\tilde{N}=344$  rad/s (\*  $s=0.1$ ,  $o^s=0.3$ )

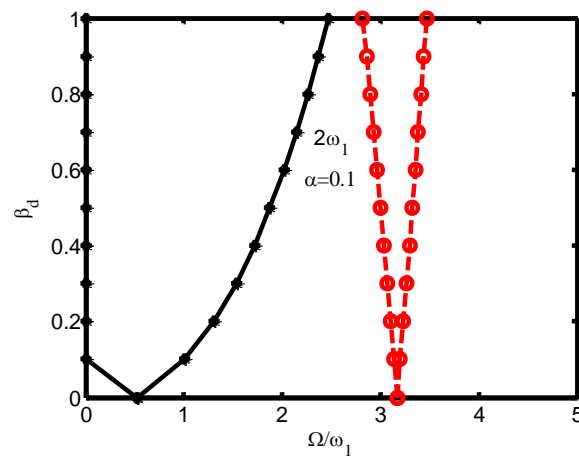


Figure 2(c). Effect of slenderness parameter on first mode instability region of steel-alumina FGO beam for exp. law,  $\delta=0.1$ ,  $\tilde{N}=344$  rad/s (\*  $s=0.1$ ,  $o^s=0.3$ )

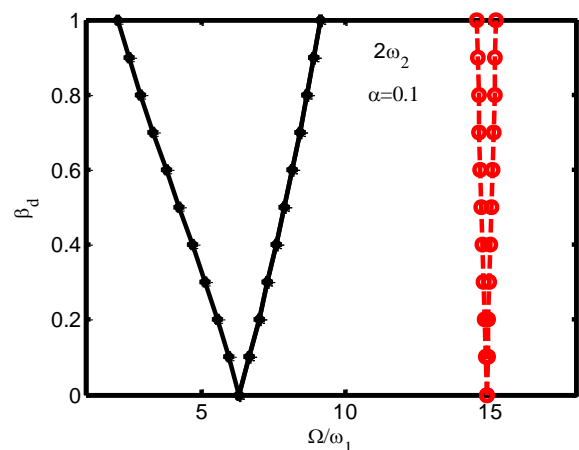
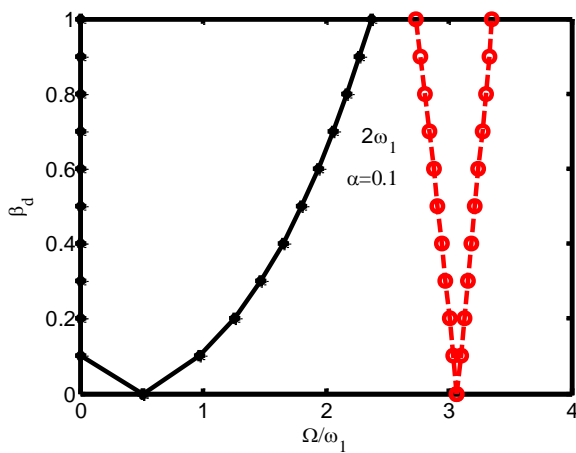


Figure 2(d). Effect of slenderness parameter on second mode instability region of steel-alumina FGO beam for exp. law,  $\delta=0.1$ ,  $\tilde{N}=344$  rad/s (\*  $s=0.1$ ,  $o^s=0.3$ )

## B. Functionally graded sandwich beam

A steel-alumina functionally graded sandwich (FGSW) rotating cantilever beam of length 1m and width 0.1m is considered for the parametric study. The bottom and top skin of the beam are steel and alumina respectively, whereas the core is the mixture of alumina and steel with bottom layer rich in steel. Both the top and bottom skin are of same thickness. The thickness of the core ( $d$ ) is 0.3 times of total thickness ( $h$ ). Figures 3(a) and 3(b) show the effect of the geometry of FGSW-2.5 beam on its first and second mode instability zones respectively. The stability of the beam is enhanced appreciably with the increase in slenderness parameter. The increase in slenderness parameter has similar effect on the instability zones of e-FGSW beam as on FGSW-2.5 beam which is shown in fig. 3(c) and 3(d) for first and second mode.



**Figure 3(a). Effect of slenderness parameter on first mode instability region of steel-alumina FGSW-2.5 beam.**

$$\delta=0.1, d/h=0.3, \tilde{N}=344 \text{ rad/s } (*^S=0.1, o^S=0.3)$$

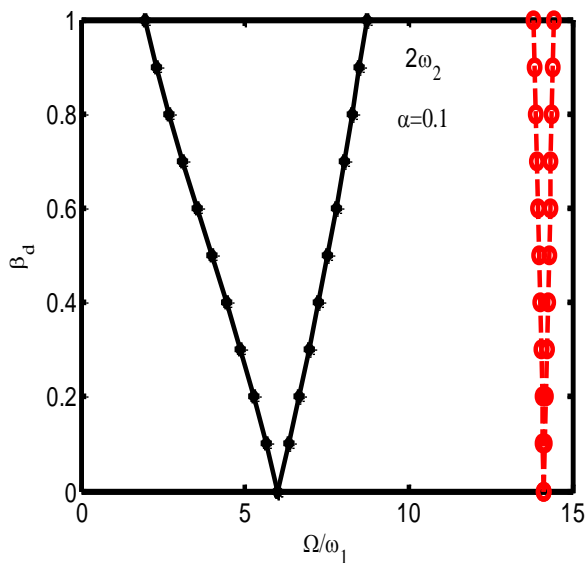


**Figure 3(b). Effect of slenderness parameter on second mode instability region of steel-alumina FGSW-2.5 beam.**

$$\delta=0.1, d/h=0.3, \tilde{N}=344 \text{ rad/s } (*^S=0.1, o^S=0.3)$$

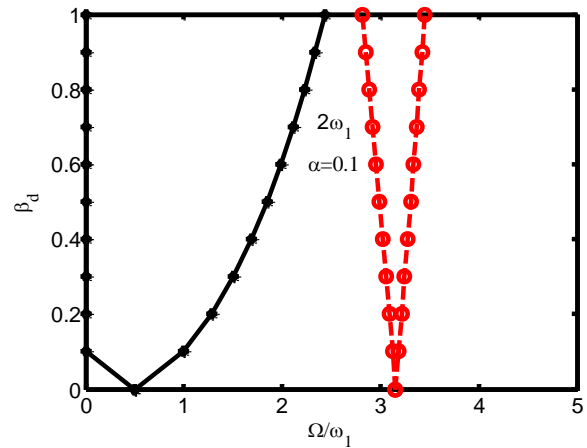


**Figure 3(c). Effect of slenderness parameter on first mode instability region of steel-alumina e-FGSW beam.**

$$\delta=0.1, d/h=0.3, \tilde{N}=344 \text{ rad/s } (*^S=0.1, o^S=0.3)$$

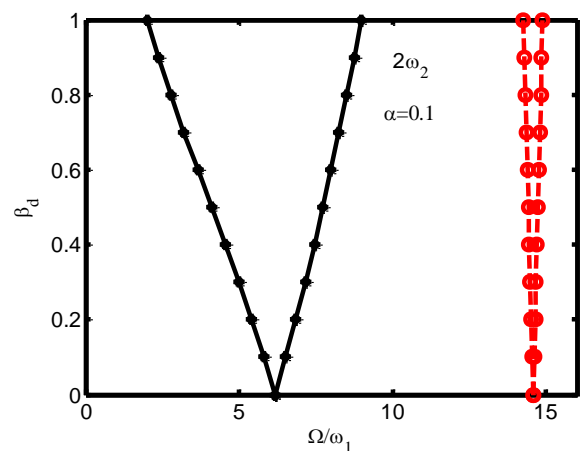


**Figure 3(d). Effect of slenderness parameter on second mode instability region of steel-alumina e-FGSW beam.**

$$\delta=0.1, d/h=0.3, \tilde{N}=344 \text{ rad/s } (*^S=0.1, o^S=0.3)$$

## V. CONCLUSION

The influence of geometry (slenderness parameter) on both functionally graded ordinary (FGO) and functionally graded sandwich (FGSW) rotating cantilever Timoshenko beams under parametric excitation have been investigated using power law ( $n=2.5$ ) and exponential law.

It has been observed that the Increase in slenderness parameter reduces the chance of parametric instability profoundly in both FGO and FGSW beams.

Application of exponential distribution ensures better dynamic stability compared to power law distribution for FGO and FGSW beams.

## REFERENCES

1. Snehshish Chakraverty, Karan Kumar Pradhan, "Vibration of Functionally Graded Beams and Plates", Elsevier, ISBN: 978-0-12-804228-1, 2016.
2. Baburaja K., Kishore D.S.C., Dasari S.R.T., Alusuri V.S., Shaik M.J., Lingineni A., Ravuri R., "Synthesis and characterization of aluminium-bamboo leaf ash metal matrix composite by stir casting technique", International Journal of Mechanical Engineering and Technology, 2017, Vol.8(5), pp:351-356.

3. Baburaja K., Teja Sainadh S., Sri Karthik D., Kuldeep J., Gowtham V., "Manufacturing and machining challenges of hybrid aluminium metal matrix composites", IOP Conference Series: Materials Science and Engineering, 2017, Vol.225(1), pp:1-9.
4. Chintalapudi B.T., Gonuguntla C.B., Pothuri M., Kant J., Pathan A., Pittala R.K., "Investigation of mechanical properties of duralumin sandwich hybrid composite using E-glass fiber", International Journal of Mechanical Engineering and Technology, 2017, Vol.8(5), pp:425-431.
5. K. S. R. Ram, B. A. Ben, C. S. RamaKrishna and K. Monika, "Fracture toughness and mechanical properties of aluminum matrix composites with fly ash as reinforcement: An industrial waste recycling", International Conference on Electrical, Electronics, and Optimization Techniques (ICEEOT), Chennai, 2016, pp. 3859-3863.
6. Baburaja K., Venkatasubbaiah K., Kalluri R., "Hybrid materials of aluminium", Materials Today: Proceedings, 2016, Vol.3(10), pp:4140-4145.
7. K.S. Raghu Ram, Sharon Rose Sweanney Bandi and Ch. Sivarama Krishna, "Mechanical Behaviour of Alumina Silicon Carbide Reinforced Particulate Reinforced Metal Matrix Composite", IOP Conference Series: Materials Science and Engineering, Volume 225, 012181, pp:1-7.
8. Mr. V. S. Jagadale, Dr. S. N. Padhi, "Mechanical Behavior of Coir Fiber Reinforced Epoxy Composites with Variable Fiber Lengths", International Journal of Innovative Technology and Exploring Engineering, Volume-8 Issue-10, 2019.
9. K.S.Raghu Ram, Deepak P.D.S.N.Ch.Siva Rama Krishna and B.Avinash Ben, "Manufacturing and Delamination Study of Drilling on Glass Fiber Reinforced Plastic (GFRP)", Australian Journal of Basic and Applied Sciences, 2015, Vol.9(36), pp: 391-395.
10. Mr. V. S. Jagadale, Dr. S. N. Padhi, "Mechanical Behavior of Coir Fiber Reinforced Polymer Resin Composites with Saturated Ash Particles", International Journal of Innovative Technology and Exploring Engineering, 2019, Vol.9(1), pp:3531-3535.
11. S.N.Padhi, K.S.Raghuram, T.Rout, V.Naga Sudha, Gill Santosh Kumar, "Mechanical Property Variation of a Rotating Cantilever FGSW Beam under Parametric Excitation", International Journal of Innovative Technology and Exploring Engineering, 2019, Vol.8(11), pp:495-499.
12. Bekir Akgöz, Ömer Civalek, "Buckling analysis of functionally graded microbeams based on the strain gradient theory", Acta Mechanica, 2013, Vol.224(9), pp: 2185-2201.
13. S.K. Jalali, M.H. Naei, A. Poorsolhjoui, "Thermal stability analysis of circular functionally graded sandwich plates of variable thickness using pseudo-spectral method", Materials & Design, 2010, Vol.31(10), pp:4755-4763.
14. S.N.Padhi, T.Rout, K.S.Raghuram, "Parametric instability and property variation analysis of a rotating cantilever FGO beam", International Journal of Recent Technology and Engineering, 2019, Vol.8(1), pp:2921-2925.
15. Liao-Liang Ke, Jie Yang, Sritawat Kitipornchai & Yang Xiang (2009) Flexural Vibration and Elastic Buckling of a Cracked Timoshenko Beam Made of Functionally Graded Materials, Mechanics of Advanced Materials and Structures, Vol.16(6), pp:488-502.
16. S.N.Padhi, G.Bhavani, V.Naga Sudha, K.S.Raghuram, T.Rout, "Effect of hub radius on rotational stability of functionally graded Timoshenko beams", International Journal of Innovative Technology and Exploring Engineering, Vol.9(1), 2019, pp:4246-4251.
17. Sid Ahmed Belalia, "Investigation of the mechanical properties on the large amplitude free vibrations of the functionally graded material sandwich plates", Journal of Sandwich Structures & Materials, 2017, Vol.21(3), pp:895-916.
18. S.C. Mohanty, R.R. Dash and T. Rout, "Free Vibration of a Functionally Graded Rotating Timoshenko Beam Using FEM", Advances in Structural Engineering, 2013, Vol.16(2), pp:405-418.
19. Yang Gao, Wan-Shen Xiao and Haiping Zhu, "Nonlinear vibration of functionally graded nano-tubes using nonlocal strain gradient theory and a two-steps perturbation method", Structural Engineering and Mechanics, 2019, Vol.69(2), pp:205-219.